Carbohydrate Polymers 114 (2014) 288–296

Contents lists available at ScienceDirect

Carbohydrate Polymers

journal homepage: www.elsevier.com/locate/carbpol

Nucleic acid delivery systems based on poly(galactosyl ureaethyl methacrylate-*b*-dimethylamino ethyl methacrylate) diblock copolymers

M.C. Munisso[a], S. Obika[b], T. Yamaoka[a,*]

[a] Department of Biomedical Engineering, National Cerebral and Cardiovascular Center Research Institute, Suita, Osaka 565-8565, Japan
[b] Graduate School of Pharmaceutical Sciences, Osaka University, Suita, Osaka 565-0871, Japan

ARTICLE INFO

Article history:
Received 12 February 2014
Received in revised form 4 August 2014
Accepted 5 August 2014
Available online 27 August 2014

Keywords:
Non-viral gene carrier
Galactosyl ureaethyl methacrylate
Antisense
Hepatocyte
PSCK9

ABSTRACT

Elevated low-density-lipoprotein cholesterol (LDL-C) level is a major risk factor leading to cardiovascular diseases. Therefore, since the proprotein convertase subtilisin kexin type 9 (PCSK9) regulates LDL-C receptors, it represents the appropriate target for cholesterol-lowering gene therapy. However, although delivery of antisense oligonucleotides (ODNs) is a promising therapeutic method for the treatment of several diseases, it is fundamental to develop new and efficacious carriers that transport the ODNs into the target cell in a nontoxic manner.

This study reports on the synthesis, characterization and in vitro testing of a new liver specific carrier based on linear cationic diblock glycopolymer composed of galactosyl ureaethyl methacrylate (GAMA) and the primary amine-containing dimethylamino ethyl methacrylate (DMAEMA). Delivery experiments proved that the poly(galactosyl ureaethyl methacrylate -b-dimethylamino ethyl methacrylate) diblock copolymer (pGa4D47), internalized in a receptor-mediated manner, exhibited a much faster nuclear transportation than ODNs carried by pDMAEMA homopolymer or glycopolymer bearing glucose moieties.

1. Introduction

Since the 1970s, gene therapy has been presented as a potential treatment for genetic disorders by replacing defective genes with DNA/ONDs molecules (Friedmann & Roblin, 1972; Zamecnik & Stephenson, 1978). However, carriers are needed to transport the DNA/ODNs through the cell membrane and to avoid degradation by nucleases, interaction with blood components, and the uptake by non-target cells. In general, viral vectors are extremely efficient carriers and may have a specific targeting ability because of their natural tendency to infect certain cell types. However, viral vectors may have oncogenic potential and can carry DNA/ODNs of limited size only. These problems can be circumvented by employing non-viral vehicles such as cationic lipids or polymers. Cationic polymers possess positive charges and can electrostatically bind to the anionic charges of DNA/ODNs to form a complex (polyplex). This action condenses the hydrodynamic radius of the polyplex and provides high flexibility with regard to the size of the DNA/ODNs that they can deliver (Wagner & Kloecker, 2006). Although non-viral carriers possess numerous advantages, several investigators have shown that their transfer efficiencies are considerably lower than those of viral vectors (Brown, Schatzlein, & Uchegbu, 2001). Therefore, improving the efficiency of non-viral vectors is essential.

Synthetic carriers may be tailored for the proposed application by choosing the appropriate molecular weight and targeting or shielding specific moieties. Ongoing research has widely demonstrated the significant influence of the polymer structure on the efficiency of gene delivery (Fischer et al., 2002; Kircheis, Wightman, & Wagner, 2001; Jeong, Song, Lim, Lee, & Park, 2001; Petersen et al., 2002; Remy et al., 1998). Thus, the carrier design requires a deep understanding of the interactions with DNA/ODNs as well as the mechanisms involved in entry in the cells. In fact, it is well-know that polyplexes are able to pass the cellular membrane via endocytosis (Merdan, Kopecek, & Kissel, 2002). Different endocytosis pathways yield different intracellular fates, which might explain why the transfection efficiency of the same carrier differs among different cell lines. The predominant entry pathway for polyplexes is adsorptive endocytosis due to the charge-mediated interaction of cationic polyplexes with negatively charged proteoglycans on

* Corresponding author. Tel.: +81 6 6833 5012x2637; fax: +81 6 6835 5476.
E-mail addresses: obika@phs.osaka-u.ac.jp (S. Obika), yamtet@ri.ncvc.go.jp, yamtet@ncvc.go.jp (T. Yamaoka).

http://dx.doi.org/10.1016/j.carbpol.2014.08.022
0144-8617/

the cell surface (Remy-Kristensen, Clamme, Vuilleumier, Kuhry, & Mely, 2001). In addition to this form of passive targeting, active targeting takes advantage of the presence on the polymer backbone of targeting moieties that specifically bind to receptors expressed on the cell surface (Fagerholm, Ortegren, Karlsson, Ruishalme, & Stralfors, 2009; Kang et al., 2010; Ning, Buranda, & Hudson, 2007; Wu & Wu, 1987, 1988). Once internalized, the polyplexes become entrapped in endosomes and are eventually transported to the lysosomes, where active enzymatic degradation processes take place. Therefore, it is essential for the polyplex to escape rapidly from the endosome and release the DNA/ODNs, which finally perform its function in the cytoplasm or nucleus.

Statins are the drugs of choice for the vast majority of patients at high risk of heart disease. However, it has been reported that patients may show side effects such as muscle pain, nausea, and liver and nervous system problems with the use of statins (Pasternak, Smith, & Bairey-Merz, 2002; Tomlinson & Mangione, 2005; Zhang et al., 2013). Therefore, it is necessary to develop new treatments to decrease the LDL-C levels. Cohen et al. (2005) demonstrated that loss-of-function mutations in *PCSK9* reduced LDL-C levels and decreased the frequency of heart disease by 88%. Thus, the use of ODNs that bind to the PCSK9 mRNA and prevents its translation, thereby inhibiting protein synthesis, appeared to be a promising approach for the cure of this pathology. The main problem lies in the safe and efficient delivery of ODNs into hepatocytes. For that reason, in the present study, we designed low-molecular-weight diblock glycopolymers as liver-targeting carriers. These vectors are composed of poly(galactosyl ureaethyl methacrylate) (GAMA), for specific gene targeting to asiloglycoprotein (ASGPR) (Wu & Wu, 1987, 1988), and dimethylamino ethyl methacrylate (DMAEMA), which is well known to possess lysosomal disruption ability via a buffering effect (Remy-Kristensen et al., 2001; van de Wetering, Cherng, Talsma, Crommelin, & Hennink, 1998; van de Wetering, Moret, Schuurmans-Nieuwenbroek, van Steenbergen, & Hennink, 1999). However, the major disadvantages of pDMAEMA-based carriers are their non-biodegradability and slight cytotoxicity. In particular, both transfection efficiency and toxicity of pDMAEMA have been reported to increase with increasing molecular weight of the cationic polymer itself (Arigita, Zuidam, Crommelin, & Hennink, 1999; Wetering, Cherng, Talsma & Hennink, 1997; Wetering, Schuurmans-Nieuwenbroek, Hennink, & Storm, 1997). Thus, in this work, considering that low-molecular-weight compounds (molecular weight lower than 30 kDa) can be excreted by the kidneys (Petersen et al., 2002), we have synthesized diblock glycopolymers with a molecular weight about 10 kDa, bearing an adequate content of galactose units to allow liver targeting and reduce the cytotoxicity. The glycopolymers were chemically characterized by proton nuclear magnetic resonance (^{1}H-NMR) and gel permeation chromatography (GPC). Polyplexes were prepared, characterized and the cytotoxicity was examined in terms of cell viability and transfection efficiency in HepG2 and HeLa cells. In addition, we used fluorescently labeled ODNs to visually study the internalization of the polyplexes into the cells.

2. Experimental

2.1. Materials

Dimethylamino ethyl methacrylate stabilized with MEHQ (DMAEMA, M_w 157.21. TCI Europe NV, Antwerp, Belgium) was used after purification. Glucosyl ureaethyl methacrylate (GUMA; Organic Chemical IND, LTD., Osaka, Japan) and galactosyl ureaethyl methacrylate (GAMA; Organic Chemical IND, LTD.) were used without further purification. *N*-*N*-dimethylformamide dehydrate (DMF; Wako, Osaka, Japan), 2-2′-bipyridyl (2-2′-bipyridine) (Bpy; Nacalai Tesque, Kyoto, Japan), copper(I) bromide (CuBr, 99.9%; Wako), copper(I) chloride (CuCl, 99.9%; Wako), and methyl (±) α-bromophenylacetate (Fluka, Tokyo, Japan) were also used without further purification.

Human hepatocarcinoma cells, HepG2, were obtained from Riken Cell Bank (Tsukuba, Japan). They were cultured in Eagle's minimum essential medium (Gibco 11995) supplemented with 10% fetal bovine serum and antibiotics/antimycotics (50 U/mL and 50 mg/mL, respectively; Gibco-Invitrogen, Carlsbad, CA). Human cervix adenocarcinoma cells, HeLa, were provided by ATCC (Tokyo, Japan). They were cultured in minimum essential medium containing non-essential amino acids (Gibco 41500-1018) supplemented with 1 mM sodium pyruvate (Gibco 1136–070), 10% fetal bovine serum, and antibiotics/antimycotics (50 U/mL and 50 mg/mL, respectively; Gibco-Invitrogen). The Lipofectamine® LTX Reagent (Life Technologies-Invitrogen, Carlsbad, CA) and linear polyethylenimine (PEI; M_w 25,000; Polysciences, Inc., Warrington, PA) were used as standard. The chemically modified 14-mer antisense phosphorothioate ODNs used in this study were synthesized by Gene Design (Osaka, Japan). The sequence used was as follows: 5′ CgTgggcagcagCC 3′; uppercase C and T indicate chemically modified 2′,4′-BNA/LNA that have a methylene bridge between the O2′ and C4′ atoms; lowercase indicates DNA (Obika et al., 1997; Singh, Kumar, & Wengel, 1998).

3. Methods

3.1. Atom transfer radical polymerization (ATRP) of diblock polymers bearing galactose or glucose moieties

3.1.1. Preparation of a macro-initiator (pGAMA or pGUMA) using GAMA or GUMA monomers

Exactly 648 mg of GUMA (0.4 M) were added to a glass tube containing 5 mL of distilled water (Scheme 1). Sixteen milligram of CuBr (0.02 M, catalyst) and 23.4 mg of Bpy (0.03 M, ligand) were added into another dried glass tube. The two tubes were then sealed with a rubber septum and bubbled with ultrahigh-purity nitrogen for 10 min. Methyl (±) α-bromophenylacetate (22.3 μL, 0.03 M, initiator) was then added via a degassed syringe to the tube contained GAMA (or GUMA) and water, and after bubbling for 10 min, the content was transferred to the tube containing the catalyst and ligand. The reaction started when the tube was transferred to an oil bath of 46 °C. The polymerization reaction was terminated after 15 min by immersing the tube into an ice water bath. The mixture was diluted with cold water and the resulting copolymers were purified using dialysis.

3.1.2. Preparation of diblock copolymers with DMAEMA monomers

First, 44 mg of pGAMA (or pGUMA, 3.8 M) was added to a glass tube containing 4 mL of DMF (Scheme 1). Then, 4.5 mg of CuCl (11.3 mM) and 11.9 mg of Bpy (19 mM) was added to a dried glass tube. The two tubes were then sealed with a rubber septum and bubbled with ultrahigh-purity nitrogen for 10 min. A monomer (DMAEMA, 477 mg, 0.76 M) was then added via a degassed syringe to the tube containing the catalyst and ligand, and after bubbling for 10 min, the content was transferred to the tube containing pGAMA (or pGUMA) dissolved in DMF. The reaction started when the tube was transferred to an oil bath of 59 °C. The polymerization was terminated after 24 h by immersing the tube into an ice water bath. The mixture was diluted with cold water and the resulting copolymers were purified by dialysis. The detailed polymerization system used in this study is listed in Table 1. The x and y of pGu_xD_y and pGa_xD_y are the polymerization degrees of GAMA (or GUMA) and DMAEMA.

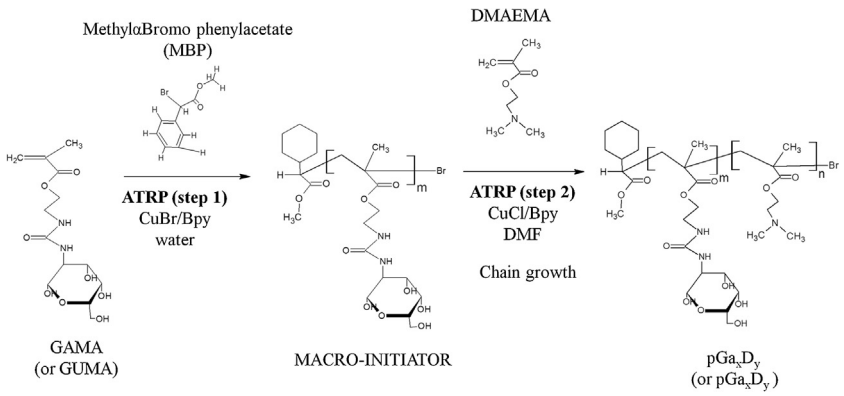

Scheme 1. Schematic representation of pGu$_x$D$_y$ and pGa$_x$D$_y$ (x is the number of GAMA or GUMA monomeric units and y is the number of the DMAEMA monomeric units).

3.2. ATRP of pDMAEMA

One gram of DMAEMA (3.18 M) was added to a glass tube containing 18 mL of ethyl 2-bromoisobutyrate (0.063 M). Then, 18.3 mg of CuBr (0.063 M) and 39 mg of Bpy (0.127 M) were added to a dried glass tube. The two tubes and an additional tube, which contained 1 mL of tetrahydrofuran, were then sealed with a rubber septum and bubbled with ultrahigh-purity nitrogen for 10 min. Tetrahydrofuran was then added via a degassed syringe to the tube containing the catalyst and ligand, and after bubbling for 10 min, the content was transferred to the tube containing DMAEMA. The reaction started when the tube was transferred to an oil bath of 46 °C. The polymerization was terminated after 2 h by immersing the tube into an ice water bath. The mixture was diluted with cold water and the resulting copolymers were purified by dialysis. The detailed polymerization system used in this study is listed in Table 1.

3.3. GPC measurement

Chromatograms for all copolymers were obtained from a conventional Shimadzu GPC system using a 0.5 M sodium acetate/0.5 M acetic acid buffer as eluent and a TSK Gel GMPWXL column (Tosoh Bioscience, Montgomeryville, PA) at room temperature and at a flow rate of 0.5 mL/min. PEI standards (M_W 400–890,000) were used for calibration.

3.4. NMR measurement

^{1}H NMR spectra of the monomers and polymers were recorded on a Varian 300 MHz Instrument (Varian Inc., Tokyo, Japan) in D_2O.

3.5. Preparation of polyplexes

Copolymer/ODN complexes differing in charge ratio but having the same ODN concentration (56 nM) were prepared as follows. Briefly, the polyplexes were prepared by adding different volumes of diblock polymer stock solution (buffer at pH 7.4) to a fixed volume of ODN stock solution in one step. After addition of the polymer solution, the dispersion was vortexed for 10 s. The polyplexes were allowed to equilibrate for 30 min at room temperature before use.

3.6. Gel retardation assay of polyplexes

ODNs were incubated with increasing amounts of diblock polymer and incubated for 20 min. Samples were electrophoresed on 1% agarose gels at 100 V for 20 min.

3.7. Heparin competition assay

The polyplexes were prepared in HEPES-buffered glucose solution (20 mM HEPES, 5% glucose w/v, pH 7.4). Different concentrations of heparin were added and the samples were electrophoresed after 30 min on 1% agarose gels at 100 V for 20 min.

3.8. Size and zeta potential of polyplexes

Dynamic light scattering measurements on polyplexes were carried out on a Malvern Zetasizer Nano ZS (Malvern, Worcestershire, U.K.) at 25 °C and at an angle of 173 degrees. The incident beam was a HeNe laser beam (633 nm). The polyplexes were prepared as described above. For calculating the z-average hydrodynamic diameter from the dynamic light scattering data, the viscosity and refractive index of HEPES-buffered glucose at 25 °C (0.89 cP and 1.333, respectively) were used. Polystyrene nanospheres (60 ± 6 nm; Duke Scientific Corp, Palo Alto, CA) were used to verify the performance of the instrument. The particle size and zeta potential of each dispersion was measured three times.

3.9. In vitro transfection and toxicity

Transfection and toxicity studies were carried out in HepG2 and HeLa cells. Transfection was carried out in 6-well plates at a density of 1.5×10^5 cells/well. Polyplexes were prepared as follows:

Table 1
Polymerization condition, characteristics, and nomenclature of polymers and block polymers synthesized via ATRP. M, I, C, L are the ratios of monomer, initiator, catalyst, and ligand, respectively. n_{DMAEMA}, m_{GAMA} and m_{GUMA} are the number of the DMAEMA, GAMA and GUMA monomeric units obtained from NMR.

Name	Solvent	M:I:C:L	Time [h]	T [°C]	M_n	M_w	PDI	Yield [%]	Composition
pGUMA	Water	20:1.5:1:1.5	0.25	50	1452	1928	1.32	42	m_{GUMA} = 4
pGU4D40	DMF	200:1:3:5	24	59	16367	31853	1.94	19.6	n_{DMAEMA} = 40
pGAMA	Water	20:1.5:1:1.5	0.25	46	2377	3630	1.52	13.6	m_{GUMA} = 4 m_{GAMA} = 5
pGA4D47	DMF	200:1:3:5	24	59	12599	24506	1.94	12.4	n_{DMAEMA} = 47
pDMAEMA	THF	50:1:1:2	2	46	8160	12486	1.53	20	m_{GAMA} = 4 n_{DMAEMA} = 42

180 μL of polymer solution in OptiMem was added to 180 μL ODN solution in OptiMem (56 nM). After incubation for 30 min at room temperature, the solution was added to the cells and the polyplexes were incubated with the cells for 5 h in both presence and absence of serum in OptiMem. After removal of the polyplex dispersion, the cells were washed with phosphate-buffered saline and fresh culture medium was added, and the cells were incubated for another 24 h. The transfection efficiency was determined by the reduction of PSCK9 gene expression using reverse transcription-polymerase chain reaction. After 24 h, the tRNA was extracted with QuickGene-Mini80 and cDNA was reverse-transcribed using High Capacity cDNA Reverse Transcription Kits (Applied Biosystems). Subsequently, TaqMan® Gene Expression Assays were performed as the second step in a two-step reverse transcription-polymerase chain reaction protocol on an ABI PRISM® and results were calculated according to the standard curve method. The transfection assays were carried out in triplicate. We used the following TaqMan probes: *Hs02758991_g1 (GAPDH)* and *Hs00545399_m1 (PCSK9)*.

A modification of the 3-(4,5-dimethyl-2-thiazolyl)-2,5-diphenyl-2*H*-tetrazolium bromide (MTT) assay was applied for estimating cell viability using a Cell Counting Kit-8 (Dojindo, Kumamoto, Japan), which contains the 2-(2-methoxy-4-nitrophenyl)-3-(4-nitrophenyl)-5-(2,4-disulfophenyl)-2*H*-tetrazolium, monosodium salt (WST-8) dye. In brief, cells were seeded at a density of 1×10^4 cells/well in 96-well Plates 24 h before the transfection. WST-8 was added 24 h after the transfection and the absorbance was measured at 450 and 600 nm using a microplate reader (Thermo Scientific Varioskan Flash, Thermo Fisher Scientific Inc. Rockford, IL USA). Experiments were performed at least six times.

3.10. Confocal microscopy

HepG2 cells were plated at a density of 1×10^4 cells/well in 96-well plates and grown for 24 h. They were incubated at 37 °C for 3 or 5 h with the polyplexes (56 nM ODNs labeled with Alexa 488 and copolymers, $N/P = 12$), followed by three washes in phosphate-buffered saline and addition of fresh medium. Cells were immediately examined with an Olympus IX81 (Olympus, Tokyo, Japan). An additional experiment was performed with an In Cell Analyzer (GE Healthcare). The cells were seeded at 1×10^4 cells/well in 96-well Plates 24 h before the transfection. Incubated at 37 °C for 2 h with the polyplexes (56 nM ODNs, $N/P = 12$), followed by three washes in phosphate-buffered saline and addition of fresh medium. ODNs were labeled with Alexa 488; nuclei were stained with Hoechst 33342, and lysosomes were stained with LysoTracker Red DND.

3.11. Statistical analysis

Results are expressed as means ± standard deviation. All statistical comparisons were made with a two-sided Student's *t*-test. A *p*-value of less than 0.01 was considered to be statistically significant.

4. Results and discussion

It is well known that pDMAEMA condenses plasmid DNA mainly through an ionic interaction and results in various transfection efficiencies depending on the polymer/DNA weight ratio (van de Wetering et al., 1997a,b). pDMAEMA is far from being the perfect antisense delivery vector. Thus, we modified its properties by adding a specific functional component: galactose moieties. Scheme 1 shows a schematic illustration of the synthetic route for pGu_xD_y and pGa_xD_y (x is the polymerization degree of GAMA or GUMA, y is the polymerization degree of DMAEMA). The diblock glycopolymer was synthesized by using two-step ATRP (Grimaud & Matyjaszewski, 1997; Percec, Barboiu, Neumann, Ronda, & Zhao, 1996; Wang & Matyjaszewski, 1995). First, we synthesized a macroinitiator (pGAMA or pGUMA), which was used as initiator in a subsequent ATRP reaction with the DMAEMA monomer. We performed a two-step reaction in order to obtain a cationic diblock glycopolymer characterized by a longer chain of pDMAEMA and a shorter chain of pGAMA (or pGUMA). For this study, three different copolymers were synthesized, as reported in Table 1. The number of repeating units was calculated by ^{1}HNMR measurements and confirmed by GPC.

According to results of the gel electrophoresis of polyplexes performed with pDMAEMA, pGa4D47, and pGu4D40 (Fig. 1(A)), an N/P ratio of 1 was sufficient for complexation and immobilization of ODNs in case of all tested copolymers. A slightly higher efficiency was detected in pDMAEMA, which showed stable polyplexes already at an N/P ratio of 0.5. The kinetics of the polyplex dissociation and the binding strength between the carrier and ODNs can be evaluated using the heparin competition assay. The results are illustrated in Fig. 1(B). Higher resistance (higher binding strength) of pDMAEMA with respect to PEI 25 k (used as control), pGa4D47, and pGu4D40 can be noted. This may be due to a better interaction of pDMAEMA with ODNs and can be interpreted as an advantage (protection of the ODNs), as well as a disadvantage (release of the ODNs). In fact, decreased ODNs release my result in decreased transfection efficiency. The size and zeta potential of the polyplexes are reported in Fig. 1(C). At N/P ratios higher than 10, the size of the different polyplexes did not show statistically significant differences with regard to the hydrodynamic diameter. All copolymers were able to complex ODNs into polyplexes with hydrodynamic diameters of 100–200 nm ($N/P > 12$). This size range is considered suitable for cellular uptake. The zeta potentials of polyplexes from diblock copolymers ranged from −40 to 30 mV, depending on the N/P ratio. No reduction in positive charge density was observed for the diblock glycopolymers (pGa4D47 and pGu4D40) in comparison to pDMAEMA. According to the measurements of the hydrodynamic diameter of polyplexes incubated in isotonic glucose and NaCl solutions, similar trends were observed for the pGa4D47-based and pGu4D40-based polyplexes () (Fig. 2). In particular, in glucose pDMAEMA-based and glycopolymer-based polyplexes showed good stability and small size over time (Fig. 2, left). Instead, in solutions of high ionic strength, although very severe aggregation was observed for pDMAEMA-based polyplexes, only small aggregates could be observed for the glycopolymers-based polyplexes. This may suggest that the galactose and glucose moieties are on the external part of the polyplexes. However, Hennink's group previously reported that the transfection efficiency of pDMAEMA polyplexes was not decreased in spite of an observed increase in size in the presence of serum (Midoux, Breuzard, Gomes, & Pichon, 2008; van de Wetering et al., 1997a,b). Thus, on the basis of these results all the carrier could be possible candidates for the transfection.

Toxicity data obtained with the WST-8 assay in HeLa and HepG2 cells (Fig. 3(A)) indicated a better biocompatibility of pGa4D47-based polyplexes compared to pDMAEMA-based and pGu4D40-based polyplexes. The transfection efficiency was evaluated as the reduction in the expression of the PCSK9 gene (Fig. 3(B)). Lipofectamine was used as control in the transfection experiments performed in the absence of serum (Fig. S1). As expected, the reduction of PCSK9 expression by Lipofectamine was very high in HeLa cells but almost ineffective in HepG2. The lower cytotoxicity and higher transfection efficiency of pGa4D47-based polyplexes compared to pDMAEMA-based polyplexes suggest that this carrier should be a good vector for in vivo experiments.

To gain detailed information on the cellular uptake of polyplexes, transfection experiments with fluorescently labeled ODNs

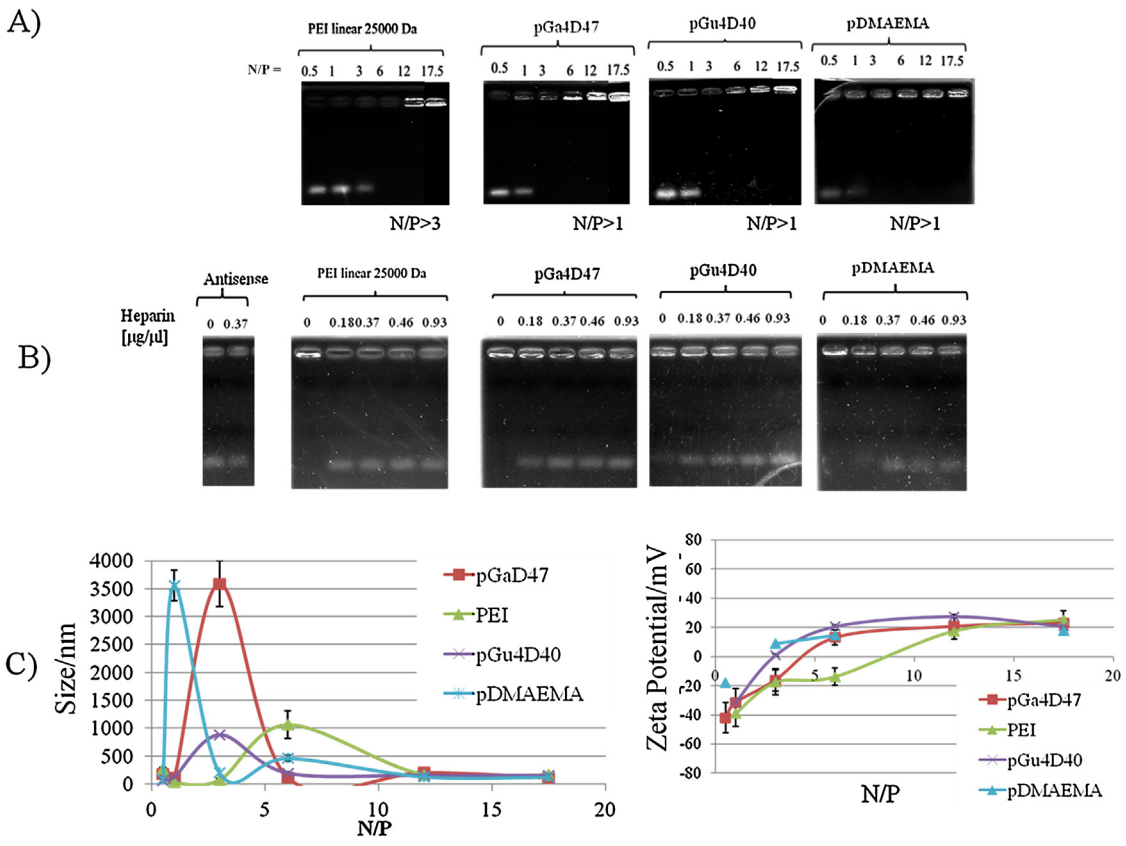

Fig. 1. (A) Gel retardation assays, (B) heparin competition assay, and (C) size and zeta potential of the polyplex (in HBG pH 7.4) are reported.

in the same cell lines were performed. The ODNs intracellular distribution at different trasfection time was characterized, by confocal microscopy, and reported in Figs. 4 and 5. From the collected images, it is possible to understand the effect of the cationic diblock glycopolymer structure on the cellular uptake and to evaluate whether ODNs are released from the carrier and is available for target message binding (Bramlage, Alefelder, Marschall, & Eckstein, 1999).

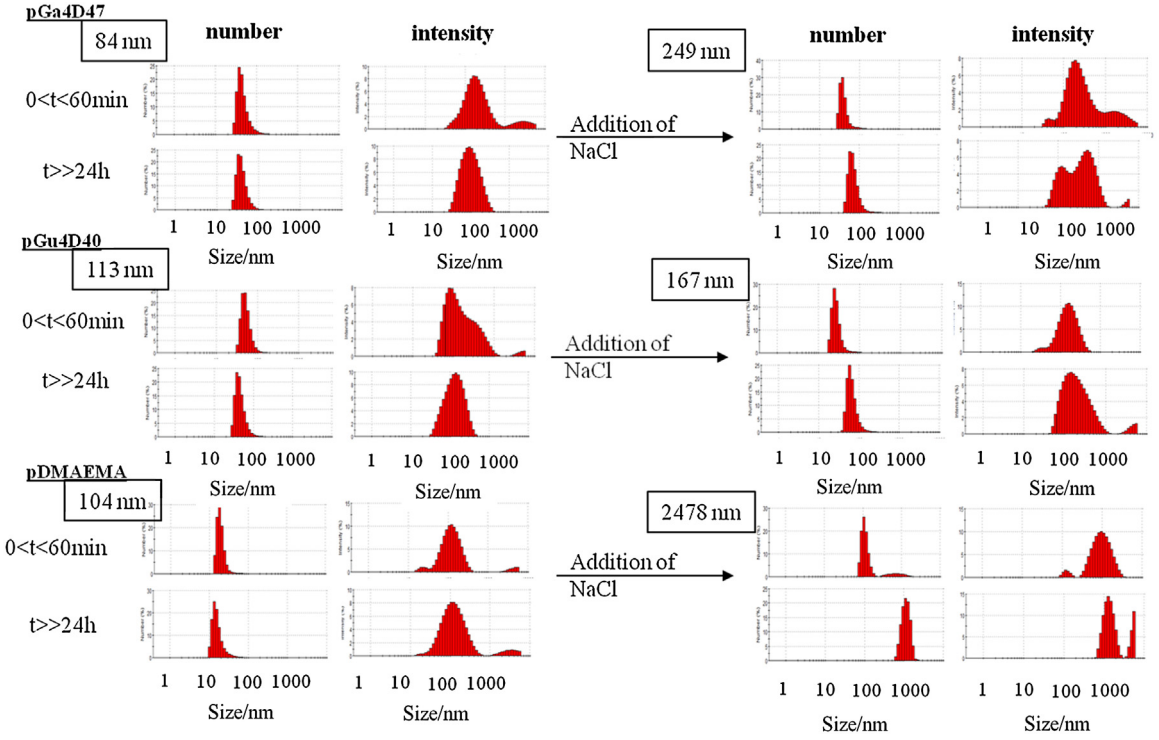

Fig. 2. Polyplex stability over time in glucose solutions (left) and isotonic salt solution (right).

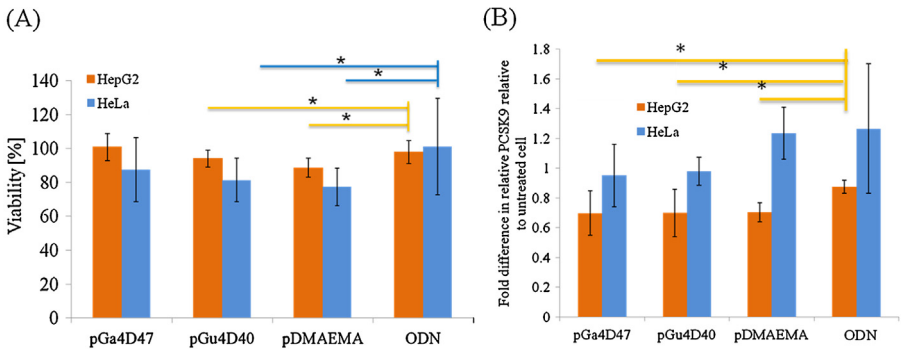

Fig. 3. (A) Toxic effect of pGa4D47, pGu4D40, pDMAEMA, and ODNs in HeLa and HepG2 cells, (B) Transfection efficiency in HepG2 and HeLa cells in the presence of 10% serum. * $p < 0.01$.

In the experiments performed in the presence of serum, after 1 h of transfection at 37 °C, Alexa 488-labeled ODNs were detected as punctated bright objects for pGu4D40-based polyplexes and as diffuse fluorescence in case of pDMAEMA-based polyplexes (Fig. 4(A)). This fluorescence was due to the attachment of the polyplexes to the cell membrane before being up taken. However, in case of pGa4D47-based polyplexes (Fig. 4(A)), fluorescence was detected in the nuclei of several cells. After 5 h, Alexa 488-labeled ODNs were also detected in the nuclei of cells treated with pGu4D40-based and pDMAEMA-based polyplexes. When the transfection was performed in serum-free medium (Fig. 4(C)), the cellular uptake was faster. In fact, after 3.25 h, it was possible to detect Alexa 488-labeled ODNs in the nuclei of several cells treated with pGu4D40-based and pDMAEMA-based polyplexes. However, cells treated with pGa4D47-based polyplexes showed nuclear uptake within 1 h. This suggests that interaction with serum proteins decreases uptake efficiency of pGu4D40-based and pDMAEMA-based polyplexes, but only partially affects pGa4D47-based polyplexes uptake. Considering that HepG2 cells have a high density of ASGPR on the cell membrane, we can conclude that the faster uptake of pGa4D47-based polyplexes might be associated with the endocytosis pathway. pGa4D47-based polyplexes are

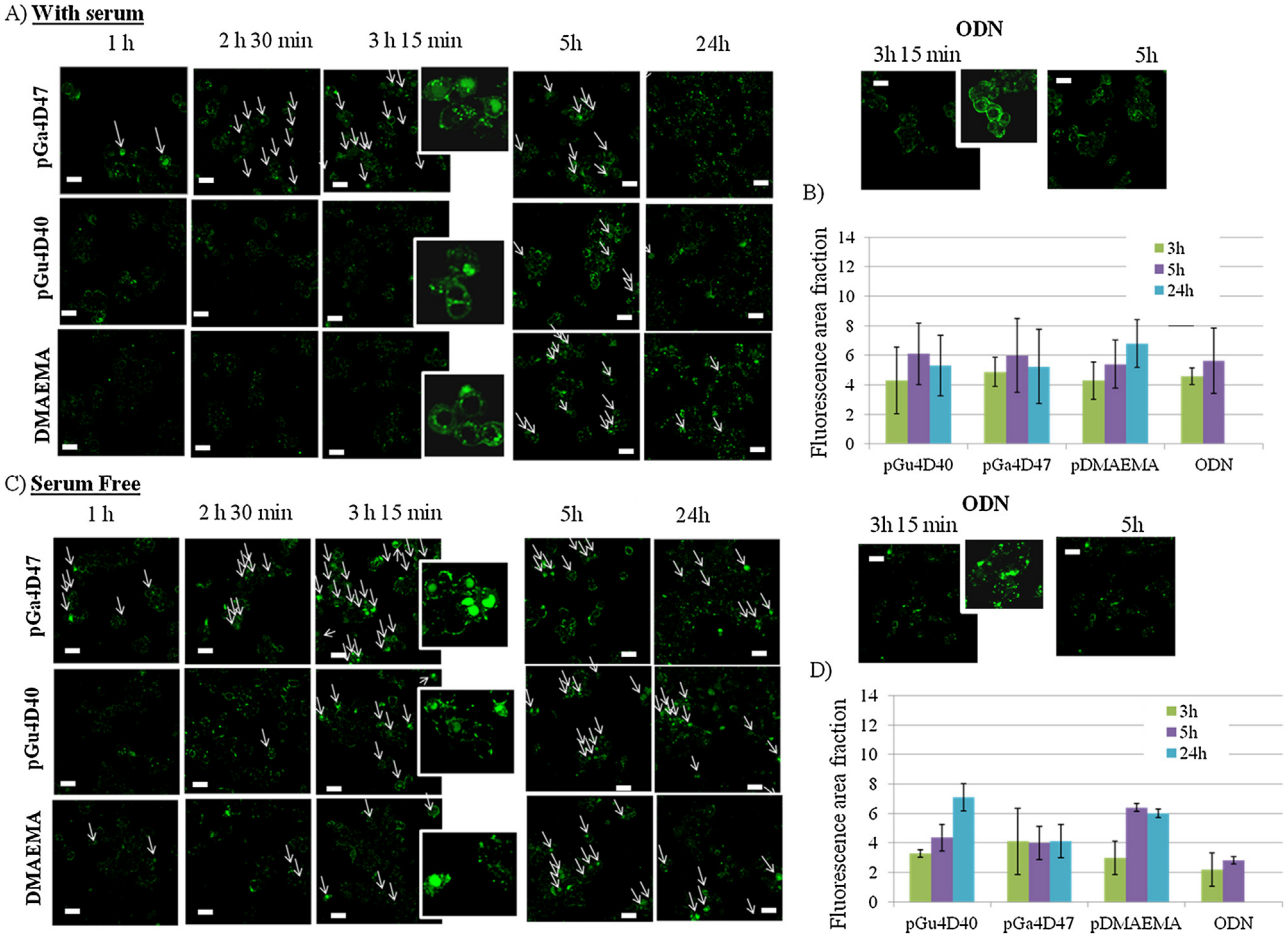

Fig. 4. Confocal microscope images collected in HepG2 cells after 1, 2.5, 3.25, 5, and 24 h of transfection with pGa4D47, pGu4D40, and pDMAEMA in the presence (A) and absence (C) of serum, respectively. Polyplexes were prepared at $N/P = 12$. White arrows indicate the diffusion in the nucleus. (B) and (D) are the fluorescence area fractions calculated using ImageJ (bar = 40 μm).

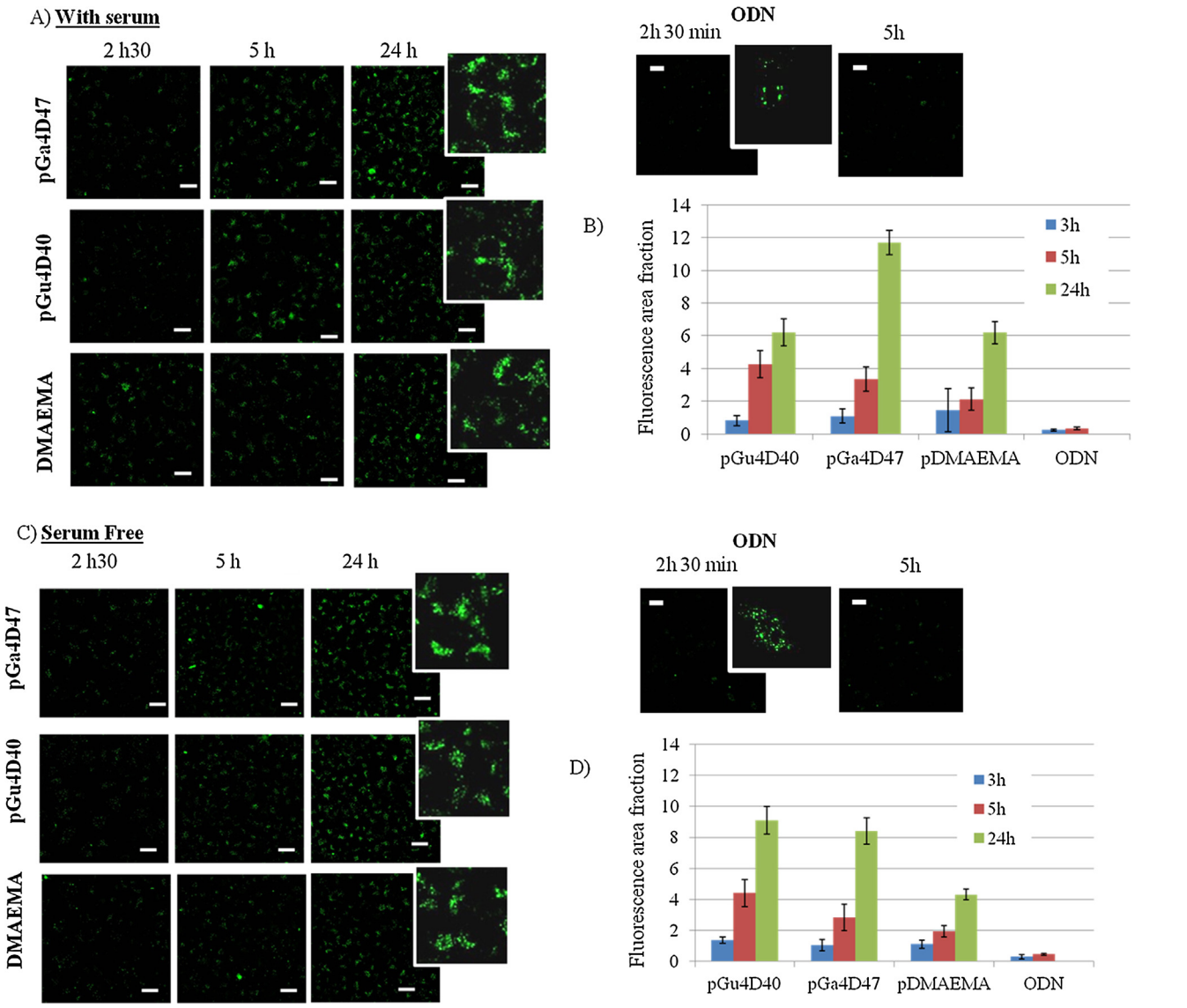

Fig. 5. Confocal microscope images collected in HeLa cells after 2.5, 5, and 24 h of transfection with pGa4D47, pGu4D40, and pDMAEMA in the presence (A) and absence (C) of serum, respectively. Polyplexes were prepared at $N/P = 12$. White arrows indicate the diffusion in the nucleus. (B) and (D) are the fluorescence area fractions calculated using ImageJ (bar = 40 μm).

taken up via adsorptive and receptor-mediated endocytosis. The latter one is a faster process because it is connected to the affinity of the ligand-receptor interaction and less affected by the presence of serum proteins. In contrast, pGu4D40-based and pDMAEMA-based polyplexes are taken up via adsorptive endocytosis, which is an interaction with generic complementary binding sites; thus, it is a slower process with higher transfection-time dependency. Indeed, in the experiments performed in the presence of serum, we noticed an increase in fluorescence emission (Fig. 4(B)) with increasing transfection time in pDMAEMA-based and pGu4D40-based polyplexes treated cells. This observation confirms that the uptake process is mainly due to adsorptive endocytosis. This phenomenon was more evident when the transfection was performed in serum-free medium (Fig. 4(D)). In the cells treated only with Alexa 488-labeled ODNs, it was possible to detect nuclear uptake in very few cases (Fig. 4, on the right), both in the presence and absence of serum. The examination of intracellular ODNs distribution (Fig. 4(A) and (C)) and results of the reverse transcription-polymerase chain reactions (RT-PCR) (Fig. S1) suggest that the entering of ODNs into the nuclei increases the transfection efficiency, but it is not a necessary phenomenon.

In the experiments performed both in the presence and absence of serum in HeLa cells (Fig. 5), a completely different behavior was observed. The cellular uptake of the Alexa488-labeled ODNs is evidently time dependent (Fig. 5(B) and (D)) for all carriers. However, no nuclear uptake was observed, even after 24 h of transfection. Despite a fluorescence emission pattern similar to that of HepG2 cells (Fig. 4(C) and (D)) after 5 h of transfection, we did not observe any reduction in the PCSK9 expression levels (Fig. 3(B)). This finding suggests that the uptake pathway in HeLa and HepG2 is very different. In fact, HeLa cell do not possess ASGPR on their cellular membrane, thus all polyplexes are taken up via the adsorptive pathway. However, the absence of a reduction in the PCSK9 expression level suggests that endosomal escape of ODNs and polyplexes may be a completely inefficient process in HeLa cells. To prove this, we collected images at the same location for 8 h post transfection by In Cell Analyzer (Fig. 6). The transfection was performed for 2 h in serum-free medium. Alexa 488-labeled ODNs are displayed in green, Hoechst 33342-stained nuclei appear blue, and Lysotracker Red DND-99-stained lysosomes appear red. In Fig. 6(B), it is clearly shown that the Alexa 488-labeled ODNs did not enter the nuclei in HeLa cells, but remained mostly in lysosomal compartments

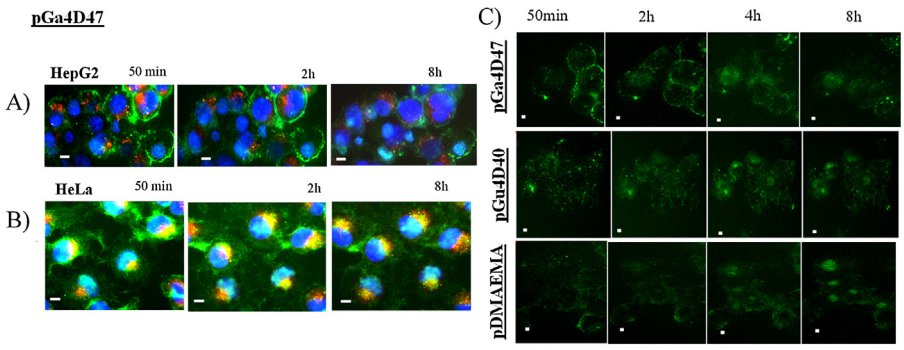

Fig. 6. Consecutive images collected with an In Cell Analyzer at different times after transfection with pGa4D47 in (A) HepG2 and (B) in HeLa cells, respectively. (C) Consecutive images collected with an In Cell Analyzer at different times after transfection in HepG2 with pGa4D47, pGu4D40 and pDMAEMA. Polyplexes were prepared at $N/P = 12$. Alexa 488-labeled ODNs are displayed in green, Hoechst 33342-stained nuclei appear blue, and LysoTracker Red DND-99-stained lysosomes appear red. Alexa488-labeled ODNs are displayed in yellow when they are inside the lysosome (bar = 6 μm). (For interpretation of the references to color in this figure legend, the reader is referred to the web version of this article.)

(Fig. 6B, yellow). In Fig. 6(A), it can be seen that the ODNs are incorporated into the nuclei (in light blue) of some HepG2 cells, and only quantity small amount remains in the endosome (in yellow). After 50 min (Fig. 6(C)), HepG2 cells treated with pGa4D47-based polyplexes showed higher accumulation of the polyplex around the cellular membrane, and the diffuse fluorescence seems to diminish with the coalescence of patches into aggregates. In HepG2 cells incubated with pGu4D40-based polyplexes, the aggregation of the polyplexes on the cellular membrane seems smaller, and several aggregates, accumulated in the inner part of the cellular membrane, can be observed. In contrast, in HepG2 cells transfected with pDMAEMA-based polyplexes, the fluorescence pattern remained diffuse and showed essentially no patching. This finding suggests that the internalization of pGa4D47-based polyplexes, and of a small amount of pGu4D40-based polyplexes, is connected to the receptor-mediated uptake. In fact, hepatocytes have cell surface receptors that recognize and bind molecules with exposed galactose, *N*-acetyl galactosamine, or glucose residues (Kim, Goto, & Akaike, 2001; Newfeld & Ashwell, 1979), even though the affinity for glucose is much lower than that for galactose. Within 2 h, the aggregates in HepG2 cells treated with pGa4D47-based polyplexes were taken up by the receptor and/or electrostatic interactions, and some Alexa 488-labeled ODNs started to enter the nucleus. A similar behavior was observed in pGu4D40-based polyplexes treated HepG2 cells. However, a diffuse fluorescence pattern was still detected in pDMAEMA-based polyplexes treated HepG2 cells. Within 4 h, nuclear accumulation appeared clearly in all HepG2 cells treated with the different polyplexes. In particular, accumulation appeared to have just started in pDMAEMA-based polyplexes treated HepG2 cells. In contrast, the results of the kinetic observations of the unfixed cells indicated that internalization in HeLa cells follows a different pathway. The polyplexes were disrupted in the lysosome (Fig. 6(B)), without entering the nucleus. A possible explanation is related to the concentration of the polyplexes and the endocytic pathway. In fact, it is possible that the carriers were not able to disrupt the endosomal membrane in HeLa cells because their concentrations were below a critical threshold value.

The increase in the transfection efficiency was not as clear as expected when using pGa4D47-based polyplexes, but this may be explained by considering the most basic assumption in ligand-receptor interactions: the ligand has to collide with the binding site of the receptor in the right orientation and remain bound long enough to stimulate endocytosis. Carbohydrate-protein interactions tend to be much weaker than protein-protein interactions; therefore, we expected that the presence of multiple units of galactose (or glucose) might enhance the affinity for ASGPR. However, this receptor clusters within sites of focal adhesion in large patches on hepatocyte membranes, and this clustering may obstruct the interaction of multiple units of sugar (Kim, Kim, & Akaike, 2003) and decrease the transfection efficiency.

In the present study, we confirmed that the cellular uptake of free ODNs is inefficient and that the fluorescence seems to be predominantly located in the endosome/lysosome. This finding is in contrast with the rapid nuclear localization of ODNs seen after complexation with pGa4D47. Our results suggest that diblock glycopolymers based on poly(galactosyl ureaethyl methacrylate) are useful gene delivery vectors; in fact, the small aggregation of the polyplexes in isotonic salt solutions and faster uptake by HepG2 cells suggest a possible high efficiency in in vivo applications. Ongoing studies on in vivo transfection experiments, characterization of the complexation, and kinetics inside the blood stream are currently under investigation.

5. Conclusion

This study demonstrates that transfection efficiency higher than that of a commercially available agent could be obtained by carefully designing the molecular structure of the diblock glycopolymeric carrier. In addition, time-course studies of the cellular uptake have proved that specific receptors can accelerate the endocytosis pathway and nuclear ODNs accumulation and, thus, increase the transfection efficiency. We have shown that transfection using these carriers in HeLa cells is inefficient because most of the ODNs are disrupted in the lysosomal compartments. This may be due to the different internalization process (non-specific endocytosis) and the low concentration of the carriers, which are not able to buffer the endosomal compartments.

However, pGaD47 could be a good carrier for in vivo experiments because of it demonstrated low toxicity, good transfection efficiency, and low aggregation in high ionic solutions.

Acknowledgments

This study was supported by the Program for Promotion of Fundamental Studies in Health Sciences of the National Institute of Biomedical Innovation (NIBIO). The authors would like to thank Dr. Atsushi Mahara, Dr. Sachiro Kakinoki, Mr. Genki Mihara, Dr. Carlos Agudelo Garcia, and Dr. Jeong-Hun Kang.

Appendix A. Supplementary data

Supplementary data associated with this article can be found, in the online version, at http://dx.doi.org/10.1016/j.carbpol.7762014.08.022.

References

Arigita, C., Zuidam, N. J., Crommelin, D. J. A., & Hennink, W. E. (1999). Association and dissociation characteristics of polymer/DNA complexes used for gene delivery. *Pharmaceutical Research*, *16*, 1534–1541.

Bramlage, B., Alefelder, S., Marschall, J. L., & Eckstein, F. (1999). Inhibition of luciferase expression by synthetic hammerhead ribozymes and their cellular uptake. *Nucleic Acids Research*, *27*, 3159–3167.

Brown, M. D., Schatzlein, A. G., & Uchegbu, I. F. (2001). Gene delivery with synthetic (non viral) carriers. *International Journal of Pharmaceutics*, *229*, 1–21.

Cohen, J. C., Pertsemlidis, A., Kotowski, I. K., Graham, R., Garcia, C. K., & Hobbs, H. H. (2005). Low LDL cholesterol in individuals of African descent resulting from frequent nonsense mutations in PCSK9. *Nature Genetics*, *37*, 161–165.

Fagerholm, S., Ortegren, U., Karlsson, M., Ruishalme, I., & Stralfors, P. (2009). Rapid insulin-dependent endocytosis of the insulin receptor by caveolae in primary adipocytes. *PLoS One*, *4*, e5985. http://dx.doi.org/10.1371/journal.pone.0005985

Fischer, D., von Harpe, A., Kunath, K., Petersen, H., Li, Y., & Kissel, T. (2002). Copolymers of ethylene imine and *N*-(2-hydroxyethyl)-ethylene imine as tools to study effects of polymer structure on physicochemical and biological properties of DNA complexes. *Bioconjugate Chemistry*, *13*, 1124–1133.

Friedmann, T., & Roblin, R. (1972). Gene therapy for human genetic disease? *Science*, *175*(4025), 949–955.

Grimaud, K., & Matyjaszewski, K. (1997). Controlled "Living" radical polymerization of methyl methacrylate by atom transfer radical polymerization. *Macromolecules*, *30*, 2216–2218.

Jeong, J. H., Song, S. H., Lim, D. W., Lee, H., & Park, T. G. (2001). DNA transfection using linear poly(ethylenimine) prepared by controlled acid hydrolysis of poly(2-ethyl-2-oxazoline). *Journal of Controlled Release*, *73*, 391–399.

Kang, J. H., Tachibana, Y., Kamata, W., Mahara, A., Harada-Shiba, M., & Yamaoka, T. (2010). Liver-targeted siRNA delivery by polyethylenimine (PEI)-pullulan carrier. *Bioorganic and Medicinal Chemistry*, *18*(11), 3946–3950.

Kim, H., Goto, M., & Akaike, T. (2001). Specific binding of glucose-derivatized polymers to the asialoglycoprotein receptor of mouse primary hepatocytes. *The Jopurnal of Biological Chemistry*, *276*(38), 35312–35319.

Kim, S. H., Kim, J. H., & Akaike, T. (2003). Regulation of cell adhesion signalling by synthetic glycopolymer matrix in primary cultured hepatocyte. *FEBS Letters*, *553*, 433–439.

Kircheis, R., Wightman, L., & Wagner, E. (2001). Design and gene delivery activity of modified polyethylenimines. *Advanced Drug Delivery Reviews*, *53*, 341–358.

Merdan, T., Kopecek, J., & Kissel, T. (2002). Prospects for cationic polymers in gene and oligonucleotide therapy against cancer. *Advanced Drug Delivery Reviews*, *54*, 715–758.

Midoux, P., Breuzard, G., Gomes, J. P., & Pichon, C. (2008). Polymer-based gene delivery: A current review on the uptake and intracellular trafficking of polyplexes. *Current Gene Therapy*, *8*, 335–352.

Newfeld, E., & Ashwell, G. (1979). Carbohydrate recognizable systems for receptor-mediated pinocytosis. In W. Lennartz (Ed.), *Biochemistry of glycoprotein and proteoglycans* (pp. 241–266). New York, NY: Plenum Press.

Ning, Y., Buranda, T., & Hudson, L. G. (2007). Activated epidermal growth factor receptor induces integrin alpha2 internalization via caveolae/raft-dependent endocytic pathway. *Journal of Biological Chemistry*, *282*, 6380–6387.

Obika, S., Nanbu, D., Hari, Y., Morio, K-i., In, Y., Inshida, T., et al. (1997). Synthesis of 2′-*O*, 4′-*C*-methylenuridine and -cydine. Novel bicyclic nucleosides having a fixed *C*-3′,-endo sugar purkering. *Tetrahedron Letters*, *38*, 8735–8738.

Pasternak, R. C., Smith, S. C., Jr., & Bairey-Merz, C. N. (2002). ACC/AHA/NHLBI clinical advisory on the use and safety of statin. *Circulation*, *106*, 1024–1028.

Percec, V., Barboiu, B., Neumann, A., Ronda, J. C., & Zhao, M. (1996). Metal-catalyzed "Living" radical polymerization of styrene initiated with arenesulfonyl chlorides, from heterogeneous to homogeneous catalysis. *Macromolecules*, *29*, 3665–3668.

Petersen, H., Fechner, P. M., Martin, A. L., Kunath, K., Stolnik, S., Roberts, C. J., Fischer, D., Davies, M. C., & Kissel, T. (2002). Polyethylenimine-graft-poly(ethylene glycol) copolymers: Influence of copolymer block structure on DNA complexation and biological activities as gene delivery system. *Bioconjugate Chemistry*, *13*, 845–854.

Remy, J.-S., Abdallah, P., Zanta, M. A., Boussif, O., Behr, J.-P., & Demeneix, B. (1998). Gene transfer with lipospermines and polyethylenimines. *Advanced Drug Delivery Reviews*, *30*, 85–95.

Remy-Kristensen, A., Clamme, J. P., Vuilleumier, C., Kuhry, & Mely, Y. (2001). Role of endocytosis in the transfection of L929 fibroblasts by polyethylenimine/DNA complexes. *Biochimica et Biophysica Acta*, *1514*, 21–32.

Singh, S. K., Kumar, R., & Wengel, J. (1998). Synthesis of 2′-amino-LNA: A novel conformationally restricted high-affinity oligonucleotide analogues with a handle. *The Journal of Organic Chemistry*, *63*, 10035–10039.

Tomlinson, S. S., & Mangione, K. K. (2005). Potential adverse effects of statins on muscle. *Physical Therapy*, *85*, 459–465.

van de Wetering, P., Cherng, J. Y., Talsma, H., & Hennink, W. E. (1997). Relation between transfection efficiency and cytotoxicity of poly(2-(dimethylamino)ethyl methacrylate/plasmid complexes. *Journal of Controlled Release*, *49*, 59–69.

van de Wetering, P., Schuurmans-Nieuwenbroek, N. M. E., Hennink, W. E., & Storm, G. (1997). Comparative transfection studies of human ovarian carcinoma cells *in vitro, ex vivo* and *in vivo* with poly(2-(dimethylamino)ethyl methacrylate)-based polyplexes. *The Journal of Gene Medicine*, *1*, 156–165.

van de Wetering, P., Cherng, J. Y., Talsma, H., Crommelin, D. J. A., & Hennink, W. E. (1998). 2-(Dimethylamino)ethyl methacrylate based (*co*)polymers as gene transfer agents. *Journal of Controlled Release*, *53*, 145–153.

van de Wetering, P., Moret, E. E., Schuurmans-Nieuwenbroek, N. M. E., van Steenbergen, M. J., & Hennink, W. E. (1999). Structure–activity relationships of water-soluble cationic methacrylate/methacrylamide polymers for nonviral gene delivery. *Bioconjugate Chemistry*, *10*(4), 589–597.

Wagner, E., & Kloecker, J. (2006). Gene delivery using polymer therapeutics. *Advances in Polymer Science*, *192*, 135–173.

Wang, J. S., & Matyjaszewski, K. (1995a). Controlled living radical polymerization—Halogen atom-transfer radical polymerization promoted by a Cu(I)Cu(II) redox process. *Macromolecules*, *28*, 7901–7910.

Wang, J. S., & Matyjaszewski, K. (1995b). Controlled/"Living" radical polymerization, atorm transfer radical polymerization in the presence of transition-metal complex. *Journal of the American Chemical Society*, *117*, 5614–5615.

Wu, G. Y., & Wu, C. H. (1987). Receptor-mediated in vitro gene transformation by a soluble DNA carrier system. *Journal of Biological Chemistry*, *262*, 4429–4432.

Wu, G. Y., & Wu, C. H. (1988). Receptor-mediated gene delivery and expression in vivo. *Journal of Biological Chemistry*, *263*, 14621–14624.

Zamecnik, P. C., & Stephenson, M. L. (1978). Inhibition of Rous sarcoma virus replication and cell transformation by a specific oligodeoxynucleotide. *Proceedings of the National Academy of Sciences of the United States of America*, *75*, 280.

Zhang, H., Plutzky, J., Skentzos, S., Morrison, F., Mar, P., Shubina, M., & Turchin, A. (2013). *Annals of Internal Medicine*, *158*(7), 526–534.